Purdue University
Purdue e-Pubs

International Refrigeration and Air Conditioning Conference

School of Mechanical Engineering

2010

Inherently Safe Looped Thermosyphon Cooling System for Aircraft Applications using Dielectric Fluid H-Galden

Ekkehard Lohse
Hamburg University of Technology

Gerhard Schmitz
Hamburg University of Technology

Follow this and additional works at: http://docs.lib.purdue.edu/iracc

Lohse, Ekkehard and Schmitz, Gerhard, "Inherently Safe Looped Thermosyphon Cooling System for Aircraft Applications using Dielectric Fluid H-Galden" (2010). *International Refrigeration and Air Conditioning Conference.* Paper 1061.
http://docs.lib.purdue.edu/iracc/1061

This document has been made available through Purdue e-Pubs, a service of the Purdue University Libraries. Please contact epubs@purdue.edu for additional information.
Complete proceedings may be acquired in print and on CD-ROM directly from the Ray W. Herrick Laboratories at https://engineering.purdue.edu/Herrick/Events/orderlit.html

Inherently Safe Looped Thermosyphon Cooling System for Aircraft Applications using Dielectric Fluid *H-Galden*

Ekkehard LOHSE[1]*, Gerhard SCHMITZ[2]

Hamburg University of Technology, Institute of Thermo-Fluid Dynamics,
Applied Thermodynamics, Hamburg, Germany
[1*]ekkehard.lohse@tu-harburg.de

Hamburg University of Technology, Institute of Thermo-Fluid Dynamics,
Applied Thermodynamics, Hamburg, Germany
[2]schmitz@tu-harburg.de

ABSTRACT

This paper presents experimental results of an inherently safe liquid cooling system. A test rig is operated at Hamburg University of Technology in order to prove the concept and gather first data for electronics cooling in modern civil aircraft. The cooling system uses a dielectric working fluid for the natural circulation in a looped thermosyphon operating in both one- and two-phase mode. First the mass flow of this natural circulation system is investigated comparing the measurement data to calculations. After that the cooling performance of the system is evaluated by taking a closer look at the heat loads and corresponding temperatures. Finally heat transfer coefficients in the cold plate are calculated. The results are discussed with respect to the following parameters, which are varied in the test series conducted: heat load, the heat sink temperature and the system orientation.

1. INHERENTLY SAFE COOLING SYSTEMS

The power densities of electronic components are increasing continuously, thus conventional air cooling systems are replaced with liquid cooling to remove the waste heat (Dietl *et al.*, 2008). Liquid cooling systems can transfer much higher waste heat flux densities. State-of-the-art liquid cooling systems use a closed cooling loop basically consisting of a cold plate and a cooler connected with pipes. The liquid is circulated by a pump. In the cold plate the waste heat from the electronic components is transferred to the working fluid. This hot liquid is pumped to the cooler, where the waste heat is discharged - in most cases to sink the ambient air acting as the final heat.

1.1 Objective in Aircraft Applications

Crucial flight systems (e.g. avionics) need highly reliable cooling systems. In common civil aircraft these systems are air cooled using forced convection. The electronics are air-ventilated by fans. Nevertheless the cooling systems are designed to ensure a minimum cooling performance without fans for some time to allow a safe landing at the nearest airport.

With increasing power densities of microprocessors and power electronics the waste heat flux densities increase and air cooling has to be replaced by liquid cooling systems like described above. The reliability is a critical issue for these active liquid cooling systems compared to the conventional air cooling. With a failure in a coolant pump, which can have many reasons, the liquid stops circulating and the electronics get overheated very quickly. Thus, analogically to air cooling, it is the aim of an inherently safe liquid cooling system to ensure a minimum cooling performance without a coolant pump. In this passive configuration the circulation of the working fluid has to be actuated by buoyancy forces, which result from density differences. In one-phase operation this is a critical issue, as the density does not vary much for most liquids. A significant change in density is achieved by evaporating the working fluid. Therefore two-phase operation is highly attractive for inherently safe liquid cooling and will be the main focus of this paper.

2. TEST RIG

The performance of an inherently safe liquid cooling system without active components is investigated experimentally using a test rig built at Hamburg University of Technology, which is described in the following. The investigations are used to prove the concept for liquid cooling systems using a dielectric working fluid - a fluorinated polyether of the *H-Galden* series by *Solvay Solexis*, which is currently used in active liquid cooling of aircraft components. As the working fluid has up to now mostly been used in one-phase applications there are only limited thermodynamical properties known, which makes it difficult, to calculate or simulate the system.

2.1 Setup

The test rig is designed as an unpressurized looped thermosyphon to cool electronic components up to a waste heat of $\dot{Q}_{\max} = 3\,\mathrm{kW}$, resulting in a maximum heat flux density of $\dot{q}_{\max} = 12.5\,\mathrm{W/cm^2}$. A schematic diagram and a photo of the test rig are shown in figure 1.

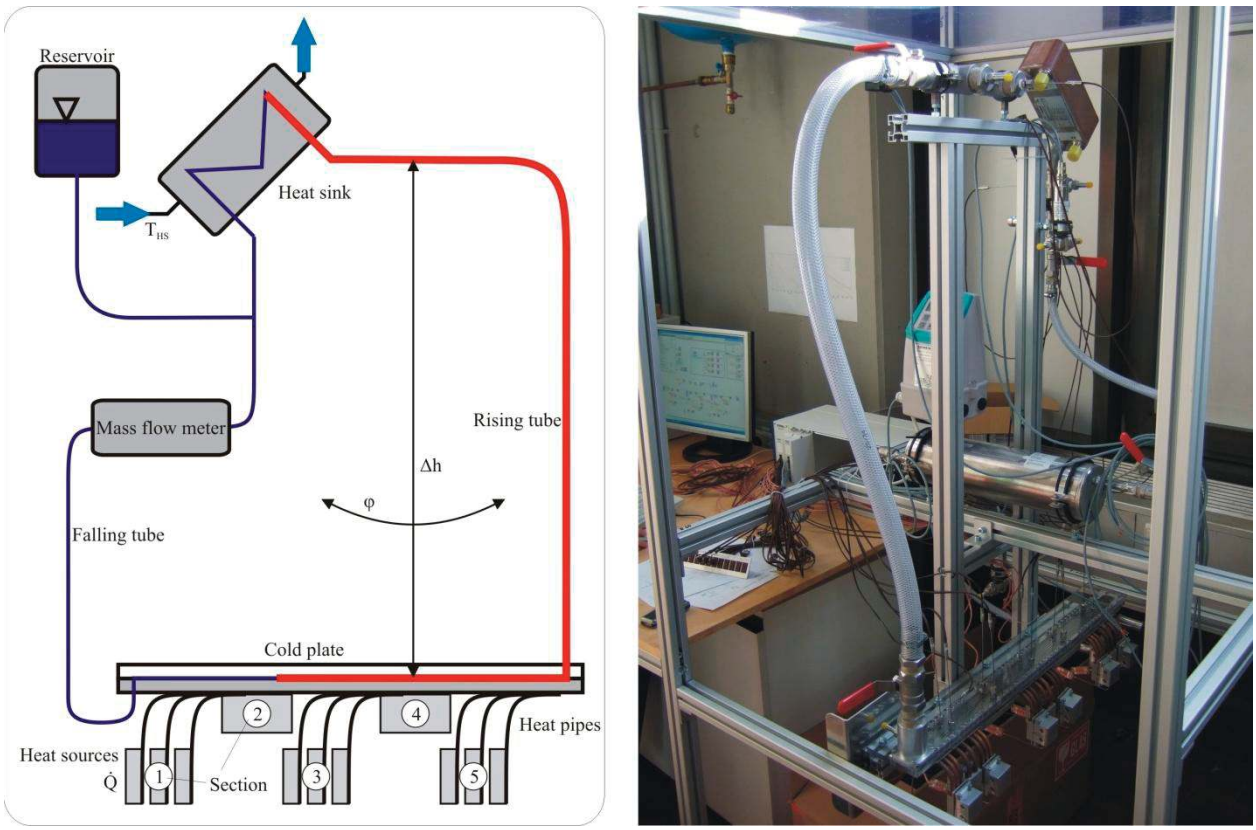

Figure 1: Test rig – schematic and photo

The components to be cooled are micro-processors, which are replaced by cartridge heaters on the test rig. In a possible aircraft application these heat sources are located on different printed circuit boards installed in a cabinet. For maintenance purposes these boards have to exchangeable. Thus the cooling loop is kept simple with a plain heat transfer surface at the bottom of the cold plate acting as thermal interface, where the circuit boards can be mounted. Inside the boards the waste heat has to be removed from the heat source and transferred to this interface, e.g. by thermal conduction. In the test rig the thermal transport is done by heat pipes. The test cold plate is divided into five sections, for which the waste heat is controlled individually. The sections 1, 3 and 5 use heat pipes as described, while in the sections 2 and 4 the waste heat sources are directly attached to the cold plate.

The main cooling loop consists of the cold plate and a heat exchanger, where the waste heat is discharged to the ambient. A cold plate is used to transfer the waste heat from the electronic components to the fluid in the cooling loop. As working fluid a fluorinated polyether of the *H-Galden ZT60* is used. It has a high density gradient in the liquid phase, which even allows one-phase operation, and evaporates at $T_{\mathrm{sat}} = 60\,°\mathrm{C}$ at ambient pressure, which allows two-phase operation of the non-pressurized cooling system to achieve high heat transfer rates. Both operation

modes are investigated experimentally. Regarding safety issues aboard commercial aircraft the fluid is dielectric, not toxic and has no flash, fire or auto-ignition point.
The hot fluid leaves the cold plate through the rising tube and is cooled down in a plate heat exchanger acting as heat sink. For natural circulation it is important, that the ambient heat exchanger is located above - with respect to gravity - the cold plate. The height difference between both heat exchangers is about $\Delta h = 1$ m. While in the test rig the heat is discharged using a vapor cycle, the final heat sink in an aircraft will be the ambient air. The sub-cooled liquid is fed back to the cold plate inlet through a separate falling tube, where a mass flow meter is integrated for testing purposes. The complete assembly is rotatable around two horizontal axes to investigate the effect of changing orientations of gravity. The top of the cold plate and most of the tubes are designed with transparent parts to observe the behavior of the two phase flow during the experiments.
The influence of three parameters on the cooling performance is investigated, which are prescribed by the boundary conditions of aircraft operation, and can all be varied independently on the test rig:

- The amount of waste heat depends on the electronics to be cooled. The number and configuration of the electronic components is given by the aircraft type and therefore depends very much on the manufacturer. On the test rig a comparably small maximum waste heat is applied just to prove the concept.
- The heat sink temperature is given by the ambient air temperature in aircraft operation. This temperature has a wide range from hot temperatures on the ground, e.g. at airports in deserts, to very cold temperatures during flight.
- The system angle is directly connected to the orientation of the aircraft. Once the orientation of all components with respect to each other is fixed, the global system angle with respect to gravity can be changed on the test rig to account for different angles of attack during flight.

2.2 Test Program

For a systematic analysis of the thermosyphon system, the variation of the three parameters is done in three test series. In each of the test series only one parameter is changed while the others are fixed. From the variation of waste heat and heat sink temperature the test matrix shown in table 1 is derived. The temperatures are varied from $T = -10$ °C to $T = 25$ °C in steps of $\Delta T = 5$ K with the waste heat set constant. The experiments are run for different waste heats. For small waste heats the cooling system works with one-phase mode. The transition heat load to two-phase operation depends on the heat sink temperature. In the observed temperature range the flow changes to two-phase around $\dot{Q} = 750$ W. In this paper only measurement data for heat loads of $\dot{Q} = 1000$ W and higher are evaluated.

Table 1: Test program – heat load and temperature variation

	Heat sink temperature							
	-10 °C	-5 °C	0 °C	5 °C	10 °C	15 °C	20 °C	25 °C
Waste heat	14 °F	23 °F	32 °F	41 °F	50 °F	59 °F	68 °F	77 °F
250 W	1-ph	1-ph	1-ph	1-ph	1-ph	1-ph	1-ph	1-ph
500 W	1-ph	1-ph	1-ph	1-ph	1-ph	1-ph	1-ph	1-ph
750 W	(2-ph)	(2-ph)	(2-ph)	(2-ph)	(2-ph)	(2-ph)	(2-ph)	(2-ph)
1000 W	x	x	x	x	x	x	x	x
1500 W	x	x	x	x	x	x	x	x
2000 W	x	x	x	x	x	x	x	x
2500 W	x	x	x	x	x	x	x	x

A cross-check with a second test series in which the waste heat is varied at a fixed heat sink temperature shows very good reproducibility of the measurement data. In a third test series the variation of the system angle is investigated. Here the waste heat and the heat sink temperature are fixed for every experiment.

3. TEST RESULTS

In this section the test results are presented and compared to theoretical analysis and literature. First the thermosyphon system is investigated focusing on the mass flow with respect to variation of the parameters. A simple

model for the theoretical prediction of the mass flow is described, using the first law of thermodynamics and common correlations for the calculation of pressure drop in pipes.
Finally the cooling performance is assessed looking at the electronics temperatures. In a more detailed analysis the heat transfer coefficients in the cold plate are calculated.

All test results presented here are acquired during test series like described above. In each test series steady states are determined and evaluated using the average values for a time span of five to ten minutes. In the following only these average values are used to describe the system behavior.

3.1 Thermosyphon System

The most interesting parameter for the natural circulation in the thermosyphon is the mass flow resulting from the waste heat applied, the heat sink temperature and the system angle.

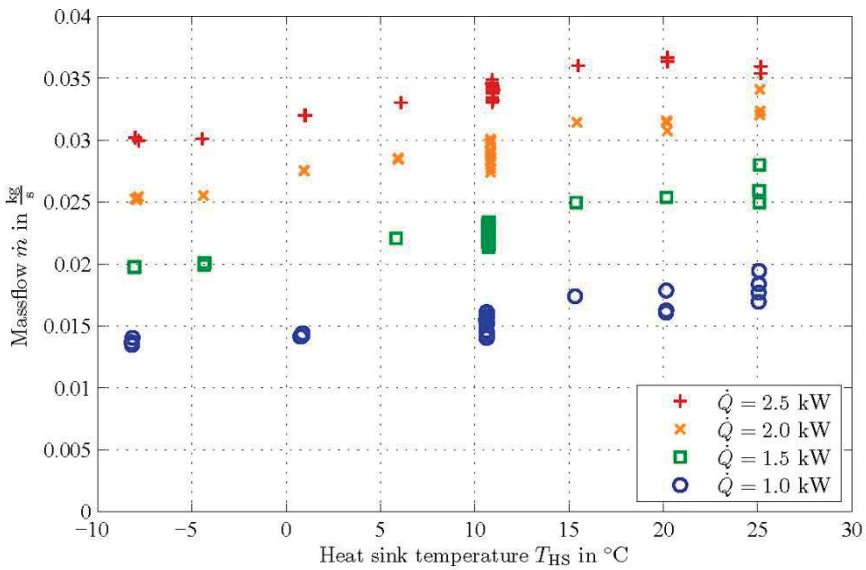

Figure 2: Mass flow with respect to heat sink temperature

Figure 2 shows the mass flow with respect to the heat sink temperature for a system angle of $\varphi = 0\,°$. Different waste heat loads are shown in different colors. As expected with higher heat loads the mass flow is increasing. In two-phase operation the mass flow increases with higher heat sink temperatures as well.
As described before, the mass flow can be predicted using a simple model based on equations given e.g. in Verein Deutscher Ingenieure (2006). The energy balance based on the first law of thermodynamics for two-phase operation is given for the cold plate by:

$$\dot{Q} = \dot{m}\left[c_{\mathrm{p}}(T_{\mathrm{out}} - T_{\mathrm{in}}) + x\,\Delta h_{\mathrm{v}}\right]$$

In the heat sink located on the top of the loop, the fluid is condensed and sub-cooled again. With the in- and outlet temperatures a mean temperature for the rising and the falling tube is calculated considering heat transfer to and from the ambient. The temperatures in the rising and falling tubes lead to different densities in the hot and cold part of the system, which are determined using the thermodynamic properties of the working fluid. From this density difference and the loops height difference the driving pressure difference is calculated:

$$\Delta p_{\mathrm{head}} = (\rho_{\mathrm{cold}} - \rho_{\mathrm{hot}})\,\Delta h\,g$$

As all geometric data of the test rig is known, the actual pressure drop in the loop is calculated with the mass flow using appropriate friction factors for the loop:

$$\Delta p_{\mathrm{loop}} = \frac{1}{2}\sum_i \rho_i\,c_i^2\,\lambda_i\,\frac{l_i}{d_i}$$

The friction factor is different depending on the flow regime: laminar or turbulent flow. The turbulent friction factor is calculated using the Blasius-correlation. In the transition a linear interpolation is used. For steady states like the

ones shown in all figures the available pressure head and the pressure drop in the loop are calculated. During the iteration the fluid temperatures, the vapor quality and the mass flow are calculated.
The results are shown in figure 3 (left) together with the experimental data plotted against the cold plate inlet temperature. The solid and dash-dotted lines are the results from the calculations for the different heat loads. The dotted lines show the theoretical mass flow calculated from the energy balance for the very beginning of two-phase flow with the fluid outlet temperature being the saturation temperature and no vapor quality at the outlet. All calculated graphs show a sharp bend and gradient change at the calculated transition temperature from one- to two-phase flow, which is also given by the intersection with the dotted lines. In one-phase operation the mass flow is nearly constant due to the temperature difference in the cold plate (cf. figure 3 top right). Here the outlet temperature rises linearly with the inlet shown for a waste heat of $\dot{Q} = 1000$ W. This results in a constant available pressure head that is shown in figure 3 (bottom right) and causes a constant mass flow.

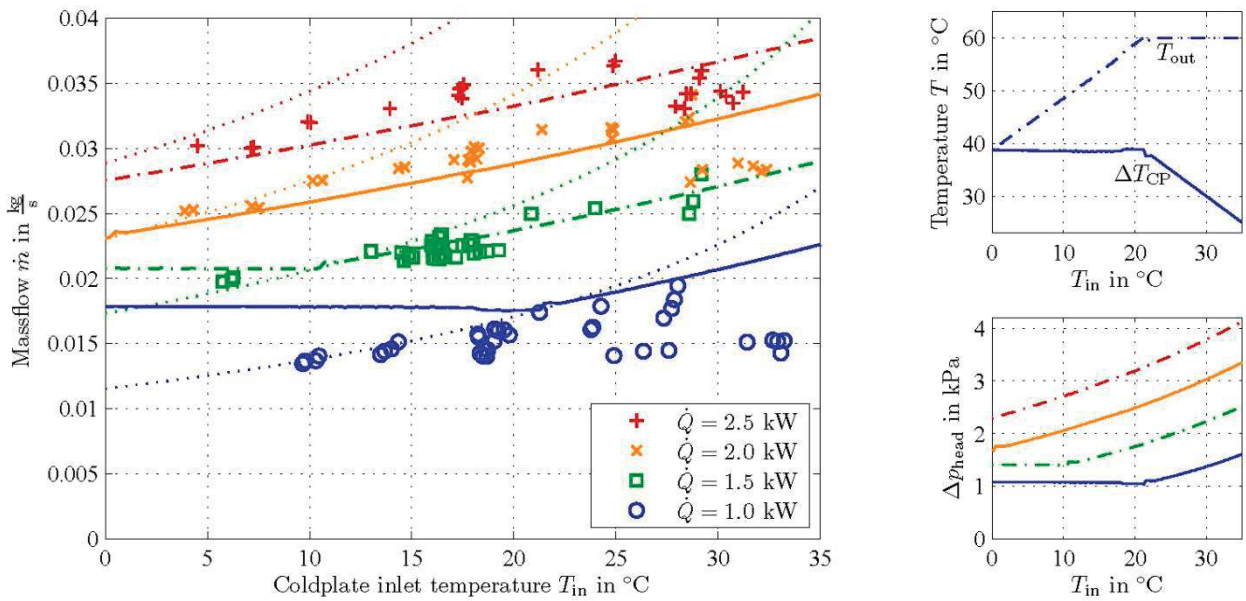

Figure 3: Mass flow – comparison of measurement and calculation

The large figure on the left also shows the experimental data matching the calculation with acceptable deviations. For high heat loads ($\dot{Q} = 2000$ W and $\dot{Q} = 2500$ W) and low temperatures the calculated values are about 10% smaller than the measured values. Only at high temperatures ($T_{in} = 30$ °C) the calculation exceeds the experimental data. For $\dot{Q} = 1500$ W the deviations are even smaller. The measurements at $\dot{Q} = 1000$ W show greater differences compared to the calculation. The solid blue line shows the calculation results. For this low heat load the calculation predicts one-phase operation up to about $T_{in} = 21$ °C, where the gradient of the graph switches. Two phase operation should occur only for higher inlet temperatures – and therefore heat sink temperatures. On the contrary the experiments show two-phase operation for lower temperatures as well.

Figure 4 shows the mass flow with respect to the system angle φ, which is varied from angle $\varphi = -10$ ° to $\varphi = +10$ °. The figure shows no significant influence on the mass flow, although the experiments show some effects regarding the flow regime. With negative system angles the mass flow shows large oscillations around a mean value that does not change significantly in the observed range. The liquid keeps the forward flow direction while the vapor fraction reverses flow in the cold plate, because of the high density and viscosity differences, and the fluid flow through pulsates. The vapor flows backwards to the upper cold plate inlet, but it cannot leave the cold plate on this end because of the construction. Therefore the vapor fills the cold plate until the pressure is high enough to push most of the vapor via the outlet into the rising tube. Subsequently the cold plate fills again with vapor until it is pushed out again. Due to this intermittent vapor flow the total mass flow has a fluctuation of about 10%, which is much more compared to zero or positive angles but has basically no effect on the cooling performance, as the heat transfer surface at the bottom is still constantly covered with liquid. The figure shows just the average mass flow values for stationary operation, which do not depend on the angle.

Another important observation is made during the start-up of the system. While for zero or positive angles the start-up works very reliable and the system always creates a mass flow without significant temperature overshoots, this does not work for negative angles. The main reason seems to be the construction and orientation of cold plate and heat sink in- and outlet, which only allow a mass flow in the design direction. For negative angles the components get superheated very quickly without generating a cooling mass-flow in the loop.

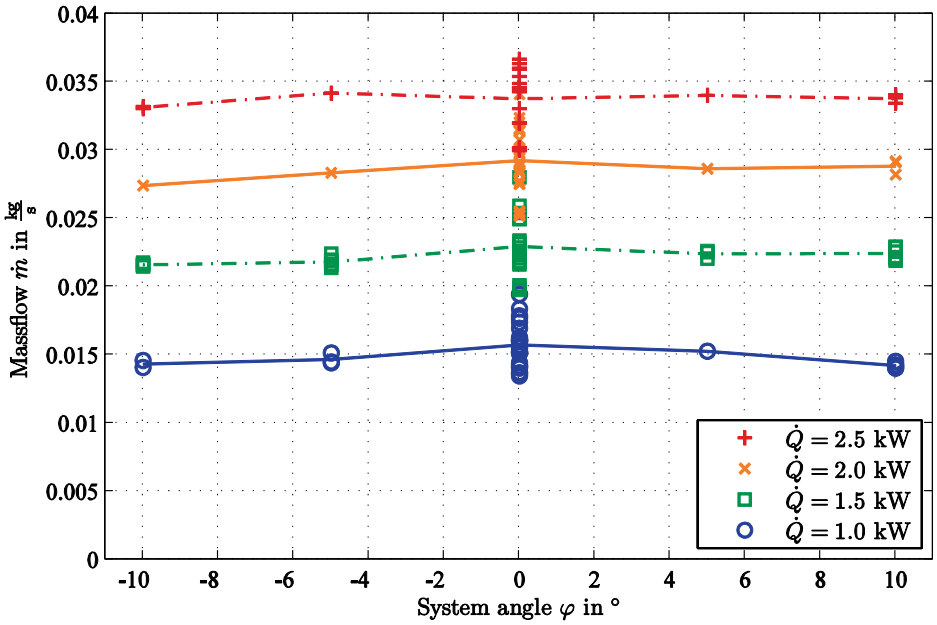

Figure 4: Mass flow with respect to system angle

3.2 Cooling Performance

Regarding the cooling performance, the mass flow described in the section above is not important, as long as the temperatures reach a steady state in which the maximum allowable temperatures are not exceeded. Therefore the cooling performance is first assessed by the electronics temperatures, which are measured in the first, middle and end section of the cold plate.

The temperatures depend on the thermal resistance between the electronic components and the fluid in the cold plate. One of the governing factors in this thermal resistance is the heat transfer coefficient in the cold plate, which is investigated at the end of this section.

The temperature limits for the electronic components to be cooled are defined by manufacturers as follows. To ensure long life-time and a high reliability the comfort temperature for continuous operation is limited to $T_{\text{comf}} = 85\,°\text{C}$. However in case of an emergency the maximum temperature is $T_{\max} = 105\,°\text{C}$, which still allows the electronics to work as designed with the drawback of reducing the life-time significantly.

The graphs in figure 5 show the measured temperatures along the cold plate for two different heat loads. On both ends the in- and outlet fluid temperatures are shown. In between the cold plate is divided into five sections, as described above, with a fluid temperature measurement (shown as "+") in each section. The fluid temperature is increasing linearly in flow direction. Due to the higher heat loads the fluid temperatures are slightly higher in the right graph.

The circles show nine temperature measurements on the heat transfer surface of the components directly attached to the cold plate in the sections 1, 3 and 5 (cf. figure 1). Both diagrams show, that the temperatures at this main interface stay within the comfort limits for continuous operation. Heat sources directly attached to the cold plate are cooled passively up to waste heat load densities of $\dot{q}_{\max} = 10.5\ \text{W/cm}^2$.

The temperature measurements shown with square markers take the thermal resistance of the heat pipes into account, as they display the temperatures directly at the heat sources. For low heat loads of $\dot{Q} = 1000$ W (left) these electronics temperatures comply with the comfort temperature limit (dashed line) only in parts, but even the highest temperatures do not exceed the maximum temperature (solid line). On the other hand these temperatures exceed the maximum temperature limit by up to $\Delta T = 45$ K for high heat loads (right), because the thermal resistance of the heat pipe assembly is too high. Experiments have shown that a significant reduction of the thermal resistance is

achieved by increasing the accuracy of the heat transfer surfaces in combination with the use of thermal greases and other thermal interface materials. The maximum temperatures at the beginning of the test series were higher than $T_{el} = 200\ °C$ which could be reduced to the temperatures shown here. Further optimization of the heat pipe assembly may very well help to increase the critical waste heat density, as the measurement data at the cold plate thermal interface show.

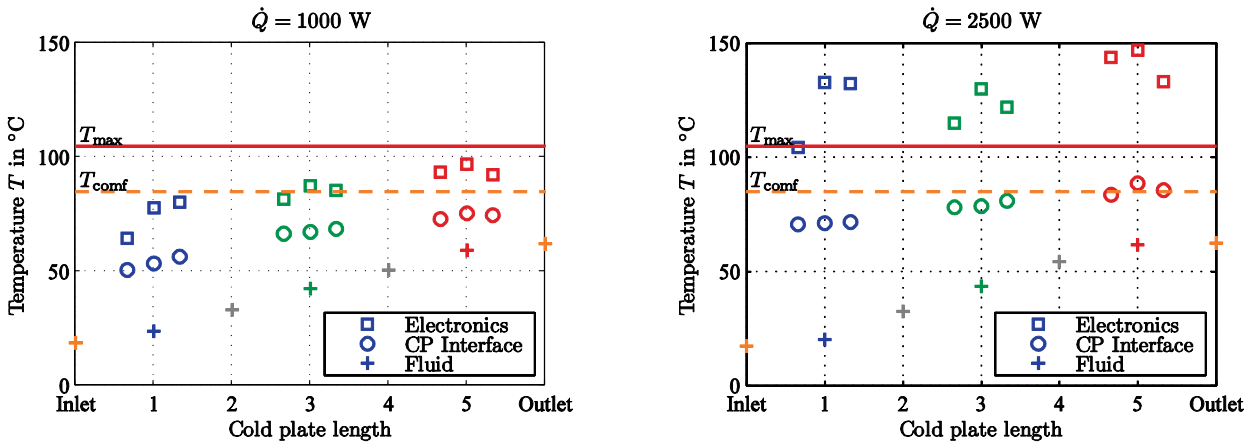

Figure 5: Temperatures along the cold plate

For the thermosyphon cooling system itself, the heat transfer from the cold plate interface into the fluid is more important. This thermal resistance is governed by the gap between components attached to the cold plate and the heat transfer coefficient from the inner cold plate wall to the fluid. For the gap smooth surfaces in combination with thermally conductive materials like foils are used. From the temperature measurement data shown above the local heat transfer coefficient is calculated for the sections 1, 3 and 5 and the mean values are plotted in figure 6 with respect to the heat load. For every section all heat transfer coefficients are plotted at one heat load to show the variance of the measurements. It has be noted, that the heat transfer coefficients increase with the heat load. The reason is the mass flow, which increases with the heat load as well (cf. figure 3). This results in higher fluid velocities which improve the heat transfer. On the other hand the heat transfer coefficients increase with the temperature and the vapor quality along the cold plate in flow direction. At the inlet the fluid is subcooled and has to be heated up to the evaporation temperature. Naturally the heat transfer coefficients for this one-phase heat transfer are lower compared to the evaporation in the last section.

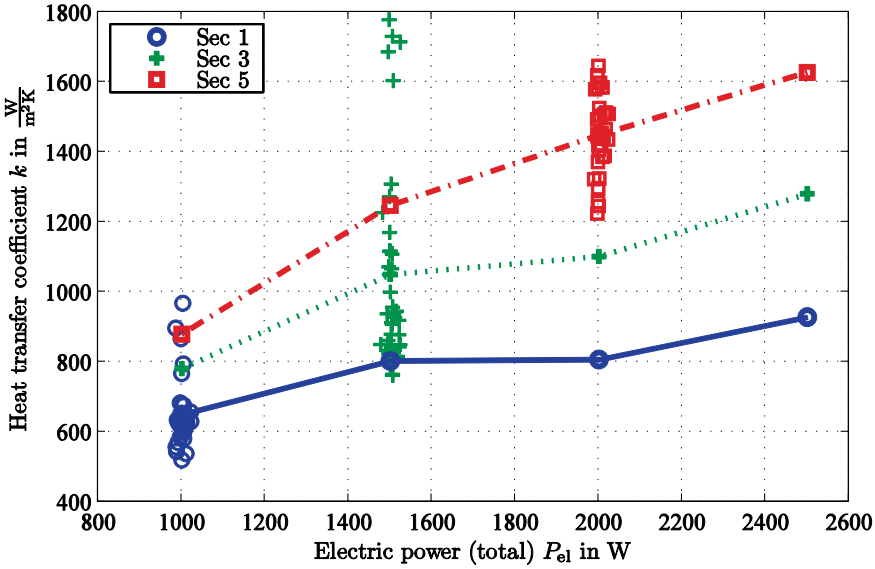

Figure 6: Heat transfer coefficient

4. CONCLUSIONS

The tests show that passive liquid cooling, operating on buoyancy forces without active components like pumps, is possible for electronic components. With the dielectric working fluid *H-Galden ZT60* common temperature limits can be maintained using the proposed system design. Additional work is needed to improve the heat transfer to the main cooling loop, while considering maintainability in aircraft applications. This will increase the operating envelope of the system with respect to the waste heat density.
The paper presents test results which show the influence of three different parameters: the heat flux density, the heat sink temperature and the system angle with respect to gravity. Measurement data for waste heat, temperatures of fluid and solid parts and mass flow are evaluated in steady state operation. The results are compared to correlations for the calculation of the thermosyphon system and state-of-the-art temperature limits.

NOMENCLATURE

The nomenclature should be located at the end of the text using the following format:

c	velocity	(m/s)
c_p	specific heat	(kJ/kgK)
d	diameter	(W)
g	gravity	(m/s²)
h	height,	(m)
Δh_v	latent heat of vaporization	(kJ/kg)
k	heat transfer coefficient	(W/m²K)
l	length	(W)
$\dot{m}$	mass flow	(kg/s)
p	pressure	(bar)
q	heat flux density	(W/cm²)
$\dot{Q}$	heat load	(W)
T	temperature	(K, °C)
x	vapor quality	(–)
λ	friction factor	(-)
φ	angle	(°)
ρ	density	(kg/m³)

Subscripts

cold	cold part
head	head
hot	hot part
HS	heat sink
in	inlet
loop	cooling loop
max	maximum
out	outlet

REFERENCES

Dietl, K., Vasel, J., Schmitz, G., *Numerical Simulation of a New Cooling System for Commercial Aircrafts*, Proceedings of the 12th International Refrigeration and Air Conditioning Conference at Purdue, 14.-17.7.2008, Purdue University, West Lafayette, USA, paper R2191

Solvay Solexis, Solvay S.A., *http://www.solvaysolexis.com/products/bybrand/brand/0,,16049-2-0,00.htm*, Manufacturer Information on the working fluid, 10.04.2010

Verein Deutscher Ingenieure, 2006, *VDI Wärmeatlas: Berechnungsblätter für den Wärmeübergang*, VDI Verlag, Düsseldorf.

ACKNOWLEDGEMENT

This work is being conducted in the frame of a project funded by the Federal Ministry of Economics and Technology (www.bmwi.de), cf. project funding reference number 20Y0803A.